Pan-Sharpening Using Induction

Muhammad Murtaza Khan, Jocelyn Chanussot
and Annick Montanvert
GIPSA-Lab–Department of Images and Signal Processing (DIS),
ENSIEG, Grenoble, France
E-mail: firstname.lastname@lis.inpg.fr

Laurent Condat
National Research Center for Environment
and Health (GSF), Dept. IBB, Munich, Germany
Email: laurent.condat@gsf.de

Abstract—**Pan-sharpening is the process of improving spatial resolution of multi-spectral (MS) satellite images using the spatial details of a high resolution Panchromatic (PAN) image. Pan-sharpening can be divided into scaling and fusion processes. In the first part of this paper we use Induction instead of bicubic interpolation for up-scaling the MS images. SFIM (Smoothing Filter based Intensity Modulation) is used to obtain fused MS images for the two different scaling techniques. In the second part, "Indusion", a new fusion technique, derived from Induction, is proposed. In this technique the high frequency content of the PAN image is extracted using a pair of up-scaling and down-scaling filters. It is then added to the up-scaled MS images. Finally a comparison of Indusion with Intensity, Hue, Saturation (IHS), Discrete Wavelet Transform (DWT) and SFIM fusion techniques is presented for IKONOS satellite images.**

I. INTRODUCTION

Current commercial satellites IKONOS and Quickbird, in the visual spectrum, provide two different types of images called Panchromatic (PAN) and Multi-spectral (MS), respectively. PAN images have a high spatial resolution but a poor spectral resolution (they are captured over a large wavelength range). On the contrary, MS images, namely red, green, blue and near-infrared, have a low spatial resolution but a high spectral resolution (they are captured over a narrow wavelength range). However, satellite images with both high spatial and spectral resolution are required to improve image interpretation and automatic classification. A high spectral resolution helps in the discrimination of land cover types, whereas a high spatial resolution helps in identifying textures or determining accurate shape and boundary of objects. Making use of PAN and MS images, Pan-sharpening aims at synthesizing MS images with a high spatial resolution [1].

Over the years different fusion techniques have been proposed, providing a compromise between the desired spatial enhancement and guarding spectral consistency. Intensity-Hue-Saturation (IHS) based methods are the most popular because of their low computational cost [2]. Together with Principal Component Analysis (PCA) based techniques [3], they fall in the category of component substitution methods. The fused images obtained by these methods have high spatial quality but they suffer from spectral distortions. SFIM fusion technique proposed by Liu [4] produces spectrally consistent fused images. However, the images obtained are blurred as compared to other fusion techniques. It was observed that this blurring was a direct result of in-accurate co-registration between the up-scaled MS and captured PAN images. This problem is related to the first phase of the fusion process, namely up-scaling of MS images. In Sect. II-B,we propose the use of the scaling technique called "Induction" [5] instead of bicubic interpolation for up-scaling the MS images. In Sect. III, "Indusion", a new fusion scheme is derived from the Induction scaling process. In Sect. IV-B, we present a quantitative comparison between different fusion techniques using the Q4 index [6]. Also, the results on IKONOS images are presented for visual analysis.

II. SFIM USING BICUBIC INTERPOLATION AND INDUCTION

A. Smoothing Filter based Intensity Modulation

SFIM [4] is based upon the idea of using the ratio between the high resolution PAN image and its low resolution image, obtained by low-pass filtering. Spatial details are injected into the up-scaled MS image, co-registered low resolution MS image without changing its spectral content as follows:

$$DN(\lambda)_{SFIM} = \frac{DN(\lambda)_{low}DN(\gamma)_{high}}{DN(\gamma)_{mean}}, \qquad (1)$$

where DN stands for "digital number", while $DN(\gamma)_{high}$, $DN(\gamma)_{mean}$, $DN(\lambda)_{low}$ and $DN(\lambda)_{SFIM}$ are the values of a pixel in high spatial resolution PAN, low spatial resolution PAN , up-scaled low spatial resolution MS and the high spatial resolution MS images, respectively. The size of the smoothing filter for obtaining the $DN(\gamma)_{mean}$ is equal to the ratio between the PAN and MS images. For the IKONOS and Quickbird satellites, this ratio is equal to 4. Hence, the used low-pass filter is a 4x4 averaging filter. However, if the up-scaled MS image is not accurately co-registered with the PAN image the fused MS image is blurred. To avoid blurring, we propose the use of Induction [5] instead of bicubic interpolation for obtaining a sharper and better co-registered up-scaled MS images.

B. Induction

Bicubic and other linear scaling techniques introduce artifacts like blurring or ringing in the up-scaled images. On the other hand, non-linear scaling techniques produce visually pleasant images, but there exists no definite relationship ensuring coherence between the initial and the enlarged images.

Induction considers magnification as the inverse problem of reduction. This yields the *reduction constraint*, stating that the enlarged image should, when reduced, give the initial image back. In [5] the authors propose a non-recursive implementation of Induction:

$$K = J + [I - [J * R] \downarrow a] \uparrow a * A. \qquad (2)$$

In the above eqn., J is an up-scaled image, obtained by using Jensen's scaling method [7]. This image does not adhere to the *reduction constraint*. I is the initial image, a is the scaling factor, R and A are the 9 and 7 tap filters of the Cohen-Daubechies-Fauveau bi-orthogonal filter pair [8] (hereafter noted as CDF 9/7). The principal idea of Induction, as defined earlier, is that an up-scaled image, when reduced, should give the initial image back. So the reduction of image J, defined in Eqn. 2 as $[J * R] \downarrow a$, should give I back. If reduction does not give the intial image I back, the difference of the two images, i.e. $I - [J * R] \downarrow a$, up-scaled and added to already up-scaled image J would result in K. Image K once reduced will respect the reduction constraint and give the initial image I back.

The CDF 9/7 filters are used in the *JPEG2000* image compression standard. The interest of using these filters for our problem is that, being symmetric, they do not cause any shift in the filtered image. It has also been proven in [8] that their smoothness and approximation properties are better than those of other filters.

III. INDUSION

In the previous subsection, we briefly described Induction. In this section, a new fusion technique is developed based upon Induction. Since the process is derived from Induction and incorporates fusion, it is baptized "Indusion". Eqn. 2 can be re-written as:

$$K = \underline{J - [[J * R] \downarrow a] \uparrow a * A} + [I] \uparrow a * A. \qquad (3)$$

The underlined part of the equation represents the high frequency content, spatial edges, while the rest of the equation represents the low frequency part of the image. J is the up-scaled version of the initial image I. Hence, the above equation represents extracting high frequency information from image J and adding it to the up-scaled low resolution image I. The idea of Pan-sharpening is to extract the high frequency information of the PAN image and add this information to the up-scaled low resolution MS image. Replacing the up-scaled image J by the PAN image and image I with the up-scaled MS image, Pan-sharpening can be obtained using Induction. The modified Indusion equation becomes:

$$K = PAN - [[PAN * R] \downarrow a] \uparrow a * A + [I] \uparrow a * A. \qquad (4)$$

Indusion algorithm was tested on IKONOS and Quickbird satellite images. Since the ratio between the PAN and MS images of these satellites is 1:4, the algorithm was divided into two stages, each with a scaling factor of 2. The Indusion algorithm is as follows:

1) Down scale PAN image from 1m to 2m resolution, $PAN_{1m} \rightarrow PAN_{2m}$, using CDF9 filter coefficients.

2) Down scale PAN image from 2m to 4m resolution, $PAN_{2m} \rightarrow PAN_{4m}$, using CDF9 filter coefficients. **Process to be repeated for each MS image:**

3) Up scale MS_{4m} image by a factor of 2 to get MS_{2m*} and scale it up again by a factor of 2 to get MS_{4m*} image, using CDF7 filter coefficients.

4) Perform histogram matching [9] between PAN_{4m} and MS_{4m}, PAN_{2m} and MS_{2m*}, PAN_{1m} and MS_{4m*} to get PAN_{HM4m}, PAN_{HM2m}, PAN_{HM1m} images.

5) Up scale PAN_{HM4m} to get PAN_{HM2m*}, using CDF7 filter coefficients.

6) Obtain the difference, $PANdiff_{HM2m}$, between PAN_{HM2m*} and PAN_{HM2m} images.

7) Add the $PANdiff_{HM2m}$ to the MS_{2m*}image. This gives us the $MS_{Fused2m}$.

8) Up scale $MS_{Fused2m}$ to get MS_{1m*}, using CDF7 filter coefficients.

9) Up scale PAN_{HM2m} to get PAN_{HM1m*}, using CDF7 filter coefficients.

10) Obtain the difference, $PANdiff_{HM1m}$, between PAN_{HM1m*} and PAN_{HM1m} images.

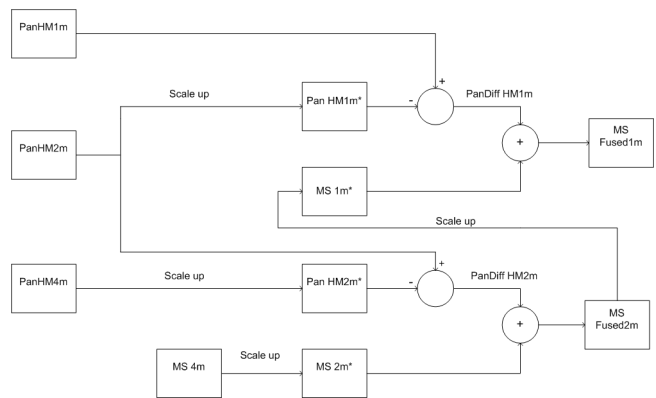11) Add the $PANdiff_{HM1m}$ to the MS_{1m*}image. This gives us the $MS_{Fused1m}$.

Fig. 1.   Indusion Process: To be repeated for each MS image

IV. EXPERIMENTAL RESULTS

A. Q4 Index

We have tested the proposed algorithm on IKONOS and Quickbird satellite images. However, before presenting the results, we need to define a quality measurement index. To cater for both spectral and radiometric distortions we have used the Q4 index [6]. This quality index is a generalization of the Q index defined in [10]. Index Q4 is for all four bands and returns a value between [0,1], with 1 indicating that the fused MS image is identical to the reference MS image. It is calculated as:

$$Q4 = \frac{|\sigma_{z1z2}|}{\sigma_{z1}.\sigma_{z2}} \cdot \frac{2\sigma_{z1}.\sigma_{z2}}{\sigma_{z1}^2 + \sigma_{z2}^2} \cdot \frac{2.|\overline{z}_1|.|\overline{z}_2|}{|\overline{z}_1|^2 + |\overline{z}_2|^2} \qquad (5)$$

where $z_1 = a_1 + ib_1 + jc_1 + kd_1$ and $z_2 = a_2 + ib_2 + jc_2 + kd_2$ This index consists of three parts. The first part consists of the

term σ_{z1z2} which is the hypercomplex covariance between $z1$ and $z2$; σ_{z1} and σ_{z2} are standard deviations. This part of the index is sensitive to loss of correlation and spectral distortions [6]. Since the quaternion can be used for all the four bands, a_1 and a_2 represent the red, b_1 and b_2 the green, c_1 and c_2 the blue and d_1 and d_2 the near infrared reference and fused images, respectively. The second term measures contrast changes while the last term measures mean bias of all bands, simultaneously. $\overline{z}_1$ and $\overline{z}_2$ are the expected values of $z1$ and $z2$. As the index is sensitive to spectral distortion, loss of correlation, changes in contrast and bias, it eliminates the need for calculating other quality measures separately. Also, with a slight variation the same measure can be used for a single band evaluation (Q1, using $z_1 = a_1$ and $z_2 = a_2$) or a three band (red, green and blue) evaluation, Q3. Before presenting the results, we need to highlight the fact that we worked on degraded spatial resolution images, PAN at 4m and MS at 16m resolution. This was done so that the resulting fused MS image has 4m resolution and can thus be compared with the original MS image serving as reference for the quality index. The reliability of this approach has been verified in [11].

B. Comparison of Fusion techniques

For the purpose of comparison, we compare Indusion with three standard algorithms: SFIM [4], fusion using DWT [12] and IHS based fusion [13]. The SFIM fusion technique was tested for both Induction scaling and bicubic interpolation. The DWT algorithm tested is referred to as the ARSIS M1 method in [11]. The implemented IHS method is described in [13]. For the quantitative analysis we present the Q3 and Q4 indices. However, we start with a visual analysis of the fused images.

Fig. 2(a) is the reference MS image and all fused images will be compared to it. The regions of interest are marked with red, blue and yellow rectangles. The red rectangle encloses a white building. Among all the fused images, the sharpest boundaries are visible in Fig. 2(b), which is the image obtained by Indusion. In Fig. 2(f) (IHS based fusion) and Fig. 2(e) (DWT based fusion), the edges of the building have changed from white to yellow, indicating spectral distortion. In Fig. 2(c),(d) (SFIM, bicubic) and (SFIM, Induction), the edges are blurred.

The blue rectangle encloses a brown building with a white circular object on it. Again, in the fused images this object is most clearly visible in Fig. 2(b). This object is not recognizable in the other fused images. The yellow rectangle encloses a building with a light green square shaped structure and two continuous lines on the right of it. The best simulation of these structures is presented by Fig. 2(f) (IHS based fusion), followed by Fig. 2(b) (Indusion) and Fig. 2(c) (SFIM Bicubic). For the other fused images, it is difficult to recognize either the continuous lines or the square shape.

As a conclusion of the visual analysis, the fused images obtained from Indusion are second only to the IHS fused images with respect to sharpness. However, the IHS fused images are spectrally distorted, whereas there is no spectral distortion in images obtained by Indusion. The images obtained from
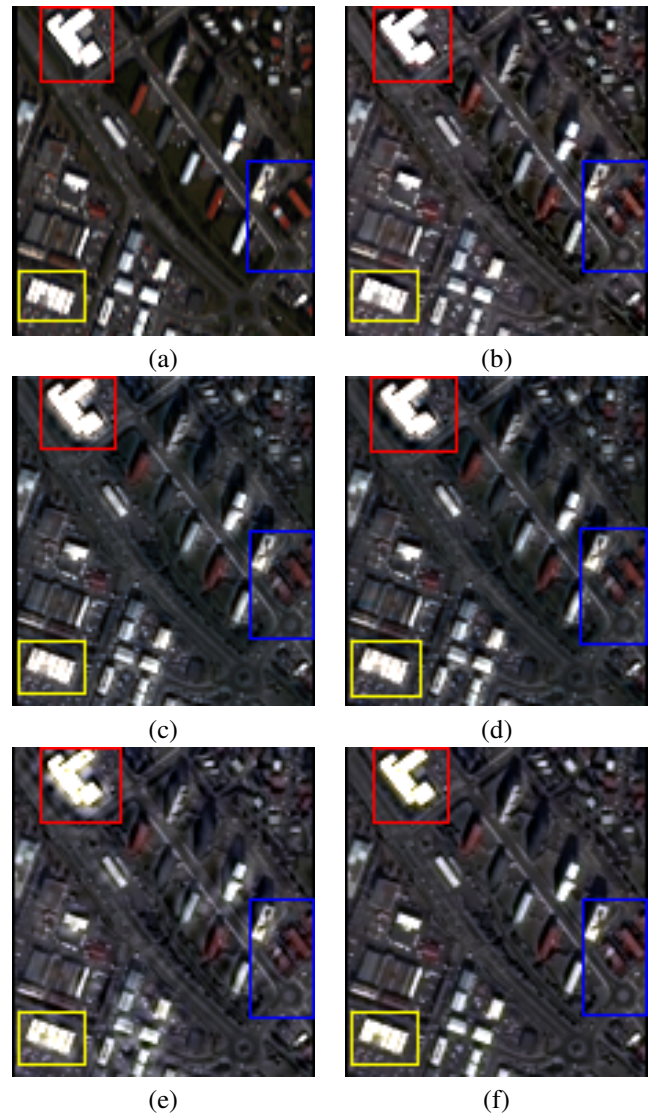

Fig. 2. Results of different fusion techniques: (a) Reference Image. (b) Indusion. (c) SFIM (Bicubic Scaling). (d) SFIM (Induction). (e) DWT. (f) IHS

SFIM and DWT algorithms are plagued by diffusion of colors around boundaries, causing blurring.

For the quantitative analysis, Q3 index presented in Tab. I, shows that the best fusion results are obtained by the Indusion algorithm (93.4% as compared to 90.6% for DWT, 88.9% for IHS and 92.9% for SFIM).

TABLE I
Q3 COMPARISON OF DIFFERENT FUSION TECHNIQUES

Fusion technique	CC: Correlation coefficients	Contrast change	Mean Bias	Q3%
	IKONOS			
SFIM (bicubic)	0.931	0.999	0.998	92.9
SFIM (Induction)	0.933	0.995	0.998	92.7
IHS	0.891	0.999	0.999	88.9
DWT	0.909	0.999	0.998	90.6
Indusion	0.936	0.999	0.998	93.4

Fusion technique	CC: Correlation coefficients	Contrast change	Mean Bias	Q4%
	IKONOS			
SFIM (bicubic)	0.924	0.999	0.998	92.2
SFIM (Induction)	0.926	0.997	0.997	92.1
IHS	-	-	-	-
DWT	0.901	0.997	0.998	89.7
Indusion	0.932	0.999	0.998	93.0

TABLE III
Q1 COMPARISON OF DIFFERENT FUSION TECHNIQUES

Fusion technique	Q1% Blue Band	Q1% NIR Band	Q1% Green Band	Q1% Red Band
	IKONOS			
SFIM (bicubic)	91.2	90.1	93.3	93.4
SFIM (Induction)	90.9	90.4	93.0	93.2
IHS	84.3	-	90.4	90.0
DWT	88.8	86.6	91.3	91.0
Indusion	92.4	91.3	93.7	93.7

A more detailed analysis also reveals that Indusion provides the best CC index. Hence, quantitatively, the image is least spectrally distorted for Indusion and most distorted for IHS. From Tab. II presenting Q4 index, one can easily conclude that the results for Indusion are again better than all the fusion algorithms tested. The IHS results are missing because the implemented IHS fusion algorithm only uses the three RGB bands for the construction of the intensity image. A further analysis of Q index for each band is shown in Tab. III.

From Tab. III, it is clear that the Q1 value for all four bands is highest for Indusion. However, when the Q1 Indusion results are compared to the SFIM bicubic results, the difference is not significant for the green and red bands. This difference is small because, unlike other bands the CC value (not given in Tab. III) of the Indusion fused red band is only slightly higher, 93.9% - 93.7% as compared to the SFIM bicubic fused band.

From Tab. I and Tab. II it is clear that SFIM renders nearly similar results for both bicubic interpolation or Induction up-scaling. This indicates that, as initially presumed, that Induction would produce better co-registered images, which are more co-related to the reference MS image, is not correct. To the contrary, we compared the up-scaled MS images with the reference MS images and found that the Q3 index was better for the images up-scaled by Induction as compared to bicubic interpolation. For the IKONOS images the difference is approximately 2% and 1% for the Quickbird satellite images. The results are shown in Tab. IV.

This leads us to conclude that a sharper up-scaled MS image does not automatically ensure a sharper and better fusion result, using the SFIM fusion algorithm. The fusion result depends upon the ratio between the high resolution PAN image and the mean PAN image. Since the mean PAN image is calculated using a 4x4 averaging filter, it can result in a slight shift of the resultant image. Hence, the ratio image would have shifted edge information and once this shifted information is added to the up-scaled MS image, the fused images are blurry.

TABLE IV
COMPARISON OF SCALING TECHNIQUES

	CC: Correlation coefficients	Contrast change	Mean Bias	Q3%
	IKONOS			
bicubic	0.850	0.980	0.998	83.2
Induction	0.860	0.994	0.998	85.3
	QuickBird			
bicubic	0.893	0.995	0.998	88.6
Induction	0.900	0.998	0.998	89.7

V. CONCLUSIONS

In this paper, the use of Induction scaling technique has been investigated in the framework of pan-sharpening. Even though it provides a better up-scaling than the standard bicubic interpolation, Induction initially did not improve the fusion results of the SFIM algorithm. In a second part, a new fusion algorithm based on Induction, called "Indusion" is proposed. It is tested on IKONOS and Quickbird data and compared with three standard methods. A visual analysis and a quantitative evaluation assess the performances of the proposed algorithm. Visually, Indusion results in sharper images as compared to the DWT based results, but slightly less sharper than the IHS results. However, the quantitative measure, QIndex, gives the best value for the Indusion algorithm. Addressing the common problem, with other algorithms, of inappropriate injection of some details is a way for key improvement in future.

REFERENCES

[1] L. Wald, *Data Fusion: Definitions and Architectures — Fusion of images of different spatial resolutions*. ENSMP, 2002.

[2] T. M. Tu, P. S. Huang, C. L. Hung, and C. P. Chang, "A fast intensity-hue-saturation fusion technique with spectral adjustment for IKONOS imagery," *IEEE Geosci. Remote Sensing Lett.*, vol. 1, no. 4, pp. 309–312, 2004.

[3] P. S. Chavez, J. Stuart, C. Sides, and J. A. Anderson, "Comparison of three different methods to merge multiresolution and multispectral data: Landsat TM and SPOT panchromatic," *Photogramm. Eng. Remote Sens.*, vol. 57, pp. 259–303, 1991.

[4] J. G. Liu, "Smoothing Filter Based Intensity Modulation: A spectral preserve image fusion technique for improving spatial details," *Int. J. Remote Sensing*, vol. 21, no. 18, pp. 3461–3472, 2000.

[5] L. Condat and A. Montanvert, "A Framework for Image Magnification: Induction Revisited," *IEEE ICASSP*, 2005.

[6] L. Alparone, S. Baronti, A. Garzelli, and F. Nencini, "A global quality measurement of pan-sharpened multispectral imagery," *IEEE Geosci. Remote Sensing Lett.*, vol. 1, no. 4, pp. 313–317, 2004.

[7] K. Jensen and D. Anastassiou, "Subpixel edge localization and the interpolation of still images," *IEEE Trans. Image Processing*, vol. 4, no. 3, pp. 265–295, 1995.

[8] M. Unser and T. Blu, "Mathematical Properties of the JPEG2000 Wavelet Filters," *IEEE Trans. Image Processing*, vol. 12, no. 9, pp. 1080–1090, 2003.

[9] D. Coltuc, P. Bolon, and J.-M. Chassery, "Exact histogram specification," *IEEE Trans. Image Processing*, vol. 15, no. 5, pp. 1143–1152, 2006.

[10] Z. Wang and A. Bovik, "A universal image quality index," *IEEE Signal Processing Lett.*, vol. 9, no. 3, pp. 81–84, 2002.

[11] C. Thomas, "Fusion d'images de résolutions spatiales différentes," Ph.D. dissertation, École des Mines de Paris, Sophia Antipolis, 2006.

[12] T. Ranchin and L. Wald, "Fusion of high spatial and spectral resolution images: The ARSIS concept and its implementation," *Photogramm. Eng. Remote Sens.*, vol. 66, no. 1, pp. 49–61, 2000.

[13] Z. Wang, D. Ziou, C. Armenakis, D. Li, and Q. Li, "A Comparative Analysis of Image Fusion Methods," *IEEE Trans. Geosci. Remote Sensing*, vol. 43, no. 6, pp. 1391–1402, 2005.